Biomass Conversion and Biorefinery (2025) 15:2131–2143
https://doi.org/10.1007/s13399-023-04325-3

ORIGINAL ARTICLE

Sorption capacity of biochars obtained by gasification of rice husks and wild sugarcane: removal of malachite green and arsenic from water solutions

Yorgelis Barría[1,2] · Aura Burbano[3] · Arthur James[1,2,4] · Gabriel Gascó[5] · Ana Méndez[6]

Received: 17 February 2023 / Revised: 2 May 2023 / Accepted: 11 May 2023 / Published online: 2 June 2023
© The Author(s) 2023

Abstract

The presence of contaminants in water has been of great concern worldwide, as it causes health risks to living organisms and general deterioration of the environment. Therefore, their elimination is essential. In the present study, rice husk (BRH) and wild sugarcane (BWS) biochars obtained by gasification were evaluated for their use as sorbents of malachite green dye (MG) and arsenite [As (III)] in aqueous solution. The chemical composition and physical structure of the two biochars were characterized by various techniques, including elemental analysis, N_2 adsorption–desorption isotherms, FTIR, and Z potential. In addition, the adsorbate removal rate was determined using the pseudo-first-order and pseudo-second-order models. Batch sorption studies were carried out to remove arsenite and MG from aqueous solutions, considering the operating parameters such as initial solution pH, temperature, contact time, concentration, and temperature. The results showed that 120 min contact time is enough to reach sorption equilibrium. The percent removal of BRH and BWS to MG was 61.99% and 97.46%, respectively, while for arsenite, it was 82.79% and 82.36%, respectively. The kinetic analysis concluded that the sorption process predominantly followed the pseudo-second-order kinetic model for both case studies since the R^2 value is approximately one. The sorption capacity calculated based on this model fitted better with the sorption capacity experimental. Finally, it was demonstrated that BRH and BWS biochars obtained as a by-product of rice husk and wild sugarcane gasification could be used as low-cost sorbent materials to remove MG dye and arsenite from an aqueous solution.

Keywords Biochar · Rice husks · Wild sugarcane · Gasification · Malachite green · Arsenic · Sorption

✉ Ana Méndez
anamaria.mendez@upm.es

1 Facultad de Ingeniería Mecánica, Universidad Tecnológica de Panamá, Panama City 0819-07289, Panama

2 Research Group—Iniciativa de Integración de Tecnologías para el Desarrollo de Soluciones Ingenieriles (I2TEDSI), Universidad Tecnológica de Panamá, Panama City 0819-07289, Panama

3 Departamento de Química, INQUISUR, Universidad Nacional del Sur (UNS) - CONICET, Av. Alem 1253, 8000 Bahía Blanca, Argentina

4 Sistema Nacional de Investigación (SNI), Clayton, City of Knowledge Edf. 205, Panama City 0819-10280, Panama

5 Departamento de Producción Agraria, E.T.S.I. Agronómica, Alimentaria y de Biosistemas, Universidad Politécnica de Madrid, Ciudad Universitaria, 28004 Madrid, Spain

6 Departamento de Ingeniería Geológica y Minera, E.T.S.I. Minas y Energía, Universidad Politécnica de Madrid, C/Ríos Rosas N°21, 28003 Madrid, Spain

1 Introduction

Water quality is affected by persistent or pseudo-persistent organic and inorganic pollutants from natural sources and anthropogenic activities. The persistence of pollutants in water sources is of great concern since they may be able to be transferred to the trophic chain, presenting a risk to the environment and human health [1, 2].

Malachite green (MG) synthetic dye is a cationic organic compound used mainly by the textile industry. Besides, MG is used as an antifungal and antibacterial agent in the aquaculture industry [3]. Discharges of untreated dye effluents pollute surface water and groundwater as dyes tend to be stable, difficult to degrade, cumulative, and toxic [4]. In addition, MG hinders the photosynthesis process in the aquatic ecosystem contributing to high chemical oxygen demand (COD) [5]. The non-biodegradable and genotoxic characteristics of the MG induce carcinogenicity and mutagenicity. In the aquaculture industry, the use of MG is not allowed in

Content courtesy of Springer Nature, terms of use apply. Rights reserved.

many countries for the treatment of food-producing animals, including the USA, the UK, China, Canada, and the European Union. However, food control authorities established a minimum required performance limit (MRPL) of 2 µg/kg of MG residues in aquaculture products and the environmental quality standard limit for the concentration of MG in water was set around 0.5–100 µg/L [6, 7].

On the other hand, toxic inorganic elements such as arsenic tend to release into the environment from the natural weathering of rocks and industrial, agricultural, and mining activities [8]. Arsenic contamination has been reported in many countries because of high concentrations in water sources. Arsenic-contaminated irrigation water represents a major risk to food safety, agricultural production, and soil contamination. Different studies have reported the bioaccumulation of arsenic in different parts of the plant, in the order roots > stem > leaves > edible parts in crops such as rice, wheat, maize, and some fruits and vegetables [9, 10]. Therefore, the recommended permissible limit of arsenic intake in drinking water as set by the World Health Organization (WHO) should be lower than 10 µg/L as a provisional guideline value [11]. Arsenic is a metalloid that can be present as arsenite [As (III)] or arsenate [As (V)]. They are more toxic and mobile than organic arsenic compounds [12, 13]. Additionally, As (III) is more difficult to remove from water than As (V) because at pH < 9 As (III) exists in the uncharged form (H_3AsO_3). The negatively charged species of As (III), including $H_2SO_3^-$, $HAsO_3^{2-}$, and AsO_3^{3-}, are found at a pH higher than 9.2. Consequently, the removal of As (III) in water by ion exchange or sorption processes is less effective than for As (V), which can exist in the form of different ions in a wide range of pHs [14, 15].

Different remediation technologies have been used for the removal of inorganic and organic pollutants present in water, such as flocculation-coagulation [16], electrochemical oxidation and photocatalytic processes[17], membrane separation [18], and phytoremediation [19], among others [20]. Currently, special attention is focused on the sorption process as a simple, efficient, and low-cost alternative for effectively remedying different contaminants in water [21]. Activated carbon is the most common and widely used sorbent for removing pollutants. However, the high production price and the use of non-renewable feedstocks have promoted the search for alternative materials of low cost and greater availability [22, 23]. Recent studies have focused on the use of different materials as potential sorbents, such as biochar, obtained by pyrolysis of industrial organic by-products of agricultural wastes, including the use of plant and animal wastes, sewage sludge, and organic municipal solid waste as materials for the removal of dyes, heavy metals, metalloids, and other contaminants [24].

Conventionally, studies have used the slow pyrolysis process to obtain biochar by thermal decomposition of biomass in an inert atmosphere [24]. Generally, biochar from gasification has not been used extensively for environmental management; its use has been studied mainly as a soil amendment agent or growing media component [25, 26]. However, the utilization of the top-lit updraft gasification process has previously been tested to produce biochar with properties for new uses [27]. Therefore, it is an alternative that can be explored to use biochar for environmental management.

The main objective of this study is to evaluate the potential of rice husk and wild sugarcane biochars obtained by the gasification process as sorbents in removing the MG and the As (III) from aqueous solutions. Rice husk is a highly available agro-industrial waste biomass; its main components are cellulose, hemicellulose, lignin, and minerals that depend on the variety of rice, climatic conditions, and geographical location of the crop [28]. In Panama, the wild sugarcane (*Saccharum spontaneum* L.) is considered an invasive species of rapid propagation and persistence since it alters the growth process of native plants [29]. In addition, other studies have focused on using wild sugarcane as an energy resource [30] or for bioremediation of groundwater contaminated with nitrate [31, 32]. Recently, biochar from wild sugarcane was evaluated for removing a synthetic herbicide (atrazine) in aqueous solutions [33].

The main objective of the present work is to study the potential use as sorbents of MG and As (III) of two biochars obtained as by-products of rice husk and wild sugarcane gasification. Batch sorption studies were carried out, and the interaction between sorbent and sorbate was evaluated using kinetic models (pseudo-first-order, pseudo-second-order) and sorption parameters.

2 Materials and methods

2.1 Sorbates

Sodium (meta) arsenite and malachite green oxalate dye with purity ≥ 90% were supplied by Sigma–Aldrich chemical company. These were used to prepare the stock solutions for the batch sorption experiments. The chemical characteristics of both sorbates are shown in Table 1.

2.2 Preparation of biochars

Two types of biomasses were selected as raw materials to produce biochar, rice husks (RH) and wild sugarcane (WS) (*Saccharum spontaneum* L.). The rice husk biomass is the agro-residual product of the company Molino el Anhelo in Panama, and the sugarcane wild was obtained from the local area in Chilibre (Panama), according to [33]. A top-lit updraft (TLUD) gasification reactor was used to carbonize the biomasses with an air supply of 16 L/min. The carbonization process used a total of 1107 g of RH and 1741 g of WS with

Content courtesy of Springer Nature, terms of use apply. Rights reserved.

Table 1 Chemical parameters of sorbates

Adsorbate	**Malachite Green oxalate**	**Sodium (meta) arsenite**
Chemical Structure	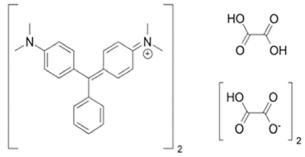	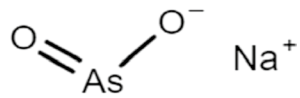
Chemical formula	$C_{52}H_{54}N_4O_{12}$	$AsNaO_2$
Weight molecular ($g \cdot mol^{-1}$)	927.02	129.91
pKa	6.90	-
K_{ow}	Not determined	-

a particle size of less than 4.75 mm. The gasification process was carried out according to previous studies [25, 34]. Reaction temperatures were measured using 2 K-type thermocouples (1/8 in. diameter) distributed along the reactor, and temperatures were recorded at a sampling rate starting from 1 s with a data acquisition system 4-channel K thermometer SD logger (88,598 AZ model, Taichung City 427, Taiwan R.O.C).

2.3 Biochar characterization

The following parameters were determined for each biochar: pH and redox potential (Eh) were determined at a dilution of 0.1:25 (g mL^{-1}) using a Crison micro pH 2000 and a pH 60 DHS, respectively [35, 36]. Ash percentage was determined by loss on ignition (LOI) method [37], and cation exchange capacity (CEC) was determined with the PerkinElmer AAnalyst 400 AA Spectrophotometer according to the standardized protocol of ISO 2347 [38]. Z potential analysis was performed using the Malvern Zetasizer Nano ZS90. C, H, N, and S contents were determined by dry combustion using a LECO CHNS 932 analyzer (SCAI-Málaga University). Oxygen was calculated by difference as 100% − (%C + %H + %N + %S + %Ash). Textural parameters of two biochars were determined by N_2 adsorption isotherms, obtained using an ASAP 2420 gas sorption analyzer from Micromeritics (SCAI-Málaga University). The sample (around 120 mg) was previously degassed under dynamic vacuum conditions to constant weight at 150 °C. The apparent specific surface area (S_{BET}) and micropore volume (S_{mic}) were obtained using the MicroActive software (v-4.03) from Micromeritics.

Finally, biochars were analyzed by Fourier transform infrared spectroscopy (FTIR) using a Bruker vertex70 FTIR spectrophotometer (SCAI-Malaga University). The measurements were carried out by transmission with the biochar power sample dispersed in KBr. A standard spectral resolution of 4 cm^{-1} in the spectral range of 4000–400 cm^{-1} and 64 accumulations per sample was used for the spectra acquisition.

2.4 Sorption studies

Sorption studies will be performed with MG and As (III) solutions.

2.4.1 Batch sorption experiments

The essential parameter to consider when designing sorption experiments is the sorption kinetics, which determines the rate at which sorption occurs. In the batch sorption kinetics study, BRH and BWS were used as sorbents of MG and As (III) in a 250-mL solution, composed of a concentration of 30 ppm of sorbate and 250 mg of each biochar, placed in a shaker in a water bath. Sorption experiments were performed at room temperature (21 °C), with controlled agitation, and carried out at the natural pH of the MG and As (III) solutions. Aliquot samples were extracted at specific time intervals of 10, 20, 30, 50, 70, and 120 min for MG and at time intervals of 10, 20, 30, 60, and 120 min for As. The final dye concentration of each aliquot was analyzed at a wavelength of 618 nm using a UV–Vis (Zuzi 4201/50 spectrophotometer), and the final As (III) concentration was quantified by ICP-MS (SCIEX Perkin Elmer model) from SCAI-Malaga University. The equilibrium sorption capacity of MG and As, q_e ($mg \cdot g^{-1}$), was calculated using Eq. 1:

$$q_e = \frac{(C_i - C_e)(V)}{W} \tag{1}$$

C_i and C_e ($mg \cdot L^{-1}$) are the liquid-phase initial and equilibrium concentrations of MG and As (III) in solution, respectively. V is the batch volume (L), and W is the mass of dry sorbent used (g).

2.4.2 Kinetic models

The sorption analysis has been carried out using kinetic models, which provide insight into the sorption pathways,

Content courtesy of Springer Nature, terms of use apply. Rights reserved.

the likely mechanisms involved, and possible rate-limiting steps. To complete this analysis concerning the possible nature of the interactions between the sorbent and the sorbate (i.e., physisorption or chemisorption), the experimental data were fitted to kinetic models such as pseudo-first- and pseudo-second-order models [39].

Pseudo-first-order (PFO) It is also known as the Lagergren model. It assumes that the rate-limiting involves the diffusion process and that the sorption kinetic depends only on the sorbate concentration. Physisorption phenomena control this model (Van der Waal forces, mechanical adhesion, and/or hydrogen bonding). The PFO equation is defined according to Eq. 2

$$\frac{dq_t}{dt} = k_1\left(q_e - q_t\right) \tag{2}$$

After integration, the linearized form of PFO is obtained according to Eq. 3:

$$\ln\left(q_e - q_t\right) = \ln q_e - k_1 t \tag{3}$$

where q_t is the sorption capacity at time t (mg·g^{-1}), q_e is the sorption capacity at the equilibrium (mg·g^{-1}), and k_1 is the rate constant of PFO (min^{-1}).

Pseudo-second-order (PSO) It assumes that the rate-limiting step is mediated by chemisorption (ion exchange, covalent forces, and/or sharing of electrons between sorbate and sorbent), which is related to sharing electrons between the surface of the sorbent and the sorbate. PSO equation is expressed according to Eq. 4:

$$\frac{dq_t}{dt} = k_2\left(q_e - q_t\right)^2 \tag{4}$$

where k_2 (g/mg·min) is the equilibrium rate constant of PSO. After the equation is integrated and considering the boundary conditions, the PFO equation is defined according to Eq. 5:

$$\frac{1}{q_t} = \left[\frac{1}{k_2 {q_e}^2}\right]\frac{1}{t} + \frac{1}{q_e} \tag{5}$$

3 Results and discussion

3.1 Physicochemical characterization and elemental composition of biochars

From the preparation of the biochars, 250 g of rice husk biochar (BRH) was obtained with a yield of 22.85%, and 250 g of biochar from wild sugarcane (BWS) with a yield of 15.74%, reaching an average maximum temperature of 1070 °C and 673 °C respectively. Table 2 shows the physicochemical properties of the two biochars. BRH and BWS exhibit alkaline pH values of 9.63 and 10.6, respectively. A high CEC value allows the retention and exchange of positively charged ions, since it influences the mobility or retention of certain contaminants. In the case of BWS, the CEC value is high value compared to BRH (346 and 99 mmolc kg^{-1}, respectively). Other studies [25, 26, 40] also reported similar pH and CEC results for biochar obtained by gasification. Furthermore, the difference between the properties of each biochar could be due to the different feedstocks and thermochemical decomposition method (oxidation rate, temperature, and thermal heating rate) since they have a substantial influence on the intrinsic properties of biochar and directly can affect the selectivity of sorbents in terms of efficiency for maximum sorbate removal [41, 42].

Table 2 shows the specific surface area of 197.64 and 16.03 m^2 g^{-1} for BRH and BWS, respectively. Additionally, the macropore volume was 3.053 and 6.84 cm^3 g^{-1} for BRH and BWS, respectively. However, BWS had a lower micropore volume than BRH. The N_2 adsorption–desorption isotherms of BRH and BWS are displayed in Fig. 1. As seen in the graphs (Fig. 1), there is a considerable difference between both isotherms. BRH showed type IV isotherms related to mesoporous development, whereas BWS behaves as type V, which is also

Table 2 Main properties, elemental analysis, and surface characteristics of biochars

Properties	BRH	BWS
pH	9.63 ± 0.05a[1]	10.6 ± 0.08b
Eh (mV)	378 ± 20b	300 ± 7a
CEC (mmol$_c$ kg^{-1})	99 ± 20a	346 ± 12b
C (%)	36.59	54.13
H (%)	0.28	1.08
N (%)	0.36	0.85
O[a] (%)	9.24	19.05
S (%)	-	0.11
H/C	0.092	0.24
O/C	0.19	0.26
(N + O)/C	0.20	0.28
Ash (%)	53.53	24.78
Specific surface area (m^2 g^{-1})	197.64*	16.03**
The total pore volume (cm^3 g^{-1})	0.096	0.012
Average pore diameter (nm)	1047	2468
Vmicro (cm^3 g^{-1})	0.0604	0.00092
Vmeso (cm^3 g^{-1})	0.035	0.012
Vmacro (cm^3 g^{-1})	3.053	6.84
Porosity (%)	80.64	88.58

[1]Values are reported as means ± standard deviation. Values in row followed by the same letter are not significantly different ($p = 0.05$) using the Duncan test

*Determined by Langmuir. **Determined by BET. [a]Calculated by difference

Content courtesy of Springer Nature, terms of use apply. Rights reserved.

associated with macroporous or non-porous materials. Differences at low relative pressures ($P/P_0 < 1$) indicated high development of microporosity in BRH compared to BWS.

3.2 Elemental analysis

The two biochars (BWS and BRH) showed different contents of oxygen (Table 2), which was higher for the BWS biochar (19.05%). Carbon content was also higher in BWS (54.13%) than in BRH (36.59%). The H/C, O/C, and (O + N)/C ratios were calculated in view of the values of C, H, O, and N in samples. BWS shows a higher H/C ratio (0.24), indicating lower aromaticity than BWS (H/C ratio of 0.09). Additionally, BWS showed slightly higher O/C and (N + O)/C values than BRH. Similar to the results obtained previously, James et al. [34] reported carbon, hydrogen, and nitrogen contents of 36.99%, 5.14%, and 0.58%, respectively, for rice husk biochar obtained in a TLUD gasifier. Similarly, Peterson and Jackson [43] used a TLUD gasifier to obtain biochar from pelletized wheat straw and corn stover with a carbon content of 74.04% and 40.66%, respectively. In addition, Hansen et al. [44] obtained less H/C and O/C atomic ratios in pine wood biochar than in wheat straw biochar, indicating increased dehydration and decarboxylation concurrently and high aromaticity and stability resulting from the carbonization process of pine wood.

3.3 FTIR analysis

FTIR analysis of two biochars was performed to characterize the surface oxygenated functional groups (Fig. 2). The two biochars show similar spectra with main differences related to the relative band intensity. The broad band centered at 3400 cm^{-1} can be attributed to -OH stretching vibrations of hydroxyl and carboxyl groups. The small bands at 2900 and 2850 cm^{-1} indicated that both materials had a low content on aliphatic structures. Their intensity was similar for the two biochars. The band centered at 1630 cm^{-1} can be ascribed to C = O vibrations in carboxylic, ester, lactones, or quinone functional groups, becoming more intense in BWS than in BHR. This result was according to high O/C content of BWS (0.26) than of BHR (0.19). Probably, the higher gasification temperature used for BHR leads to the loss of some oxygenated groups. The slight band at 1380 cm^{-1} can be related to C-O in phenolic and ether groups and the presence of C-N groups. This band is more intense for BWS. Additionally, the broadband between 1000 and 1200 cm^{-1} can be attributed to C-O bonds due to the presence of alcohols (C-O) and aliphatic ethers (C–O–C). Finally, Si–O stretching can be observed in this FTIR region, indicating the presence of SiO_2.

3.4 XRD analysis

Figure 3 shows the XRD analysis of the two biochars, BRH and BWS. The intensity of the diffraction beam has been expressed as a function of 2 theta. As can be seen in the graph, BRH and BWS are amorphous in nature, showing a broad band between 15 and 25° characteristic in these materials. On the other side, BWS also exhibits the crystallographic planes 28 and 40° that can indicate the presence of calcite that does not decompose during gasification at 673 °C.

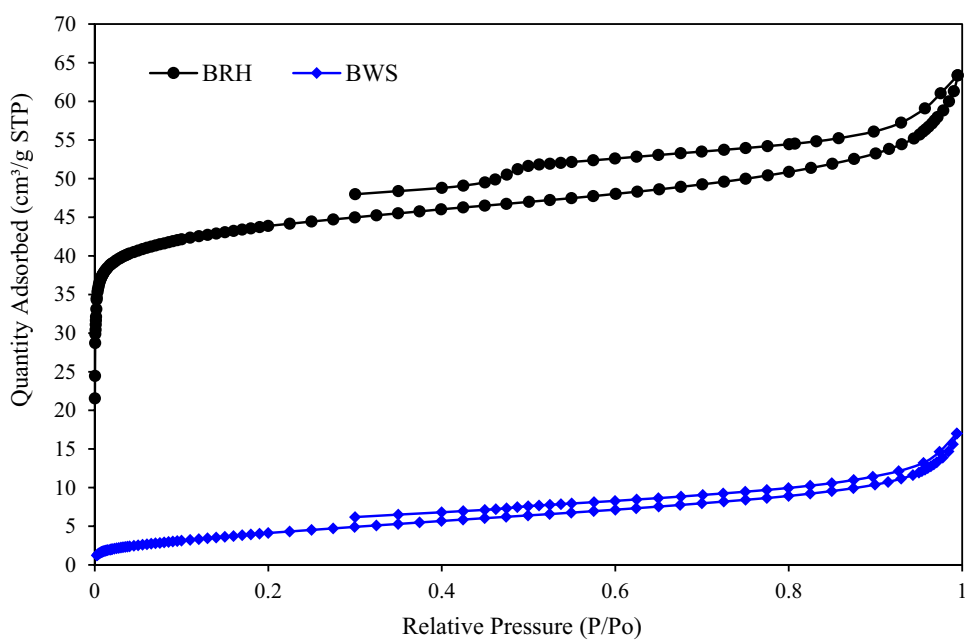

Fig. 1 N_2 adsorption–desorption isotherms of biochars BRH and BWS

Content courtesy of Springer Nature, terms of use apply. Rights reserved.

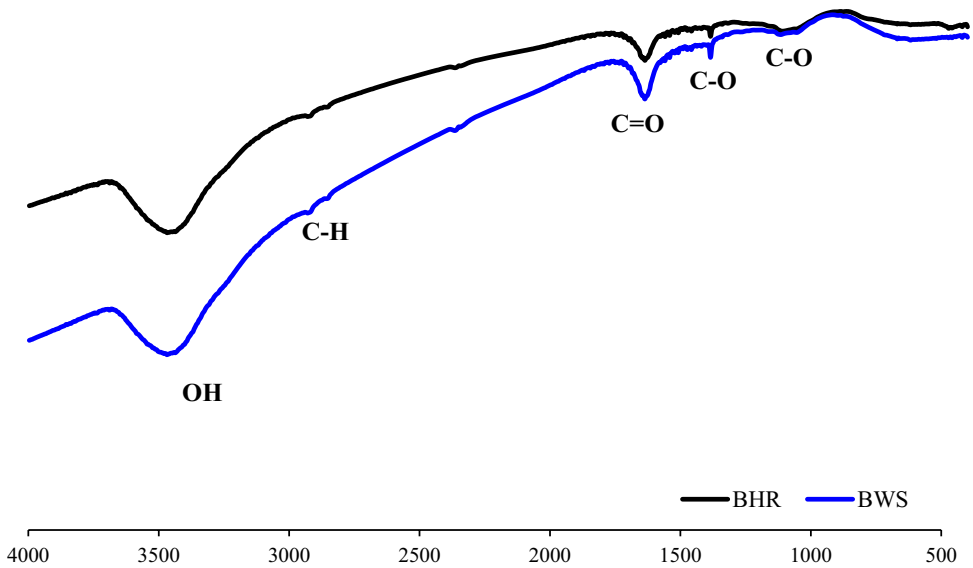

Fig. 2 FTIR spectra of biochars BHR and BWS

3.5 Zeta potential

Zeta potential (electro potential kinetics in colloidal systems) is the potential that is formed between the biochar and the medium. This potential provides important information about the behavior of the materials and stability in an aqueous solution. A large positive or negative Z potential indicates good stability of the suspensions due to repulsion between particles. Figure 4 depicts the zeta potential as a function of the pH of BRH and BWS. Both materials show a negative Z potential in the utilized pH range, highlighting that BWS presents the most negative Z potential in magnitude.

3.6 Batch sorption kinetic studies

The kinetic study allows identifying the possible sorption mechanisms and the effect of the contact time in the process, which is necessary to evaluate the sorption efficiency of the dye. The influence of the biochars BRH and BWS on the removal of MG and As (III) was analyzed in terms of contact time at intervals of 10 min up to 120 min, at an initial concentration of 30 mg L^{-1} of the dye (MG), 250 mg of each biochar, room temperature (21 °C), constant agitation, and with an initial pH of 4.88 MG/BRH, 9.63 As/BRH, 9.95 MG/BWS, and 10.50 As/BWS for the solution.

Figure 5 shows that the equilibrium state was established at 120 min when the removal of MG and As (III) was kept constant. A 97.46% removal of MG dye was obtained using BWS, and a 61.99% removal of MG dye using BRH. Furthermore, it was observed that more than 90% of MG removal occurred in the first 10 min when using BWS, as opposed to using BRH. The great affinity of BWS by MG can be related to high functionality, high negative

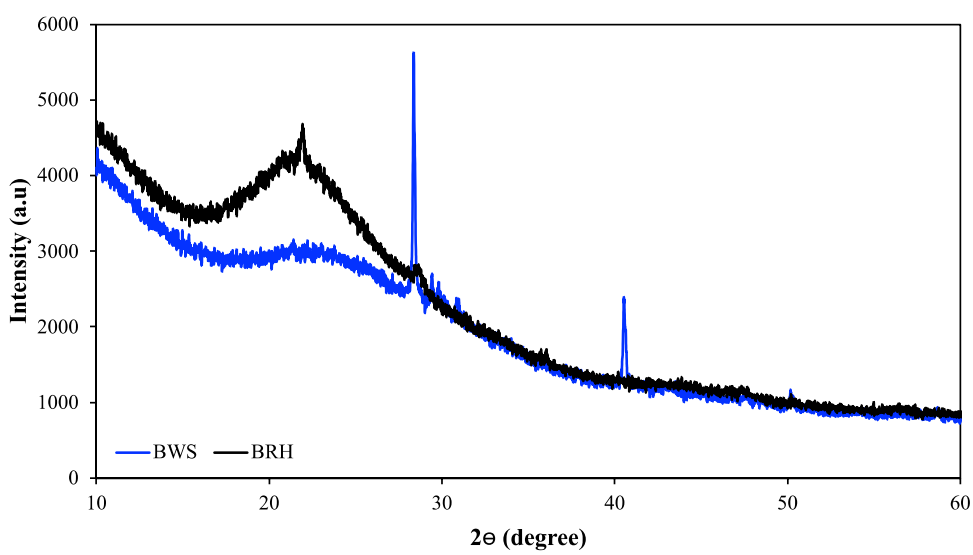

Fig. 3 X-ray diffraction pattern of biochars BRH and BWS

Content courtesy of Springer Nature, terms of use apply. Rights reserved.

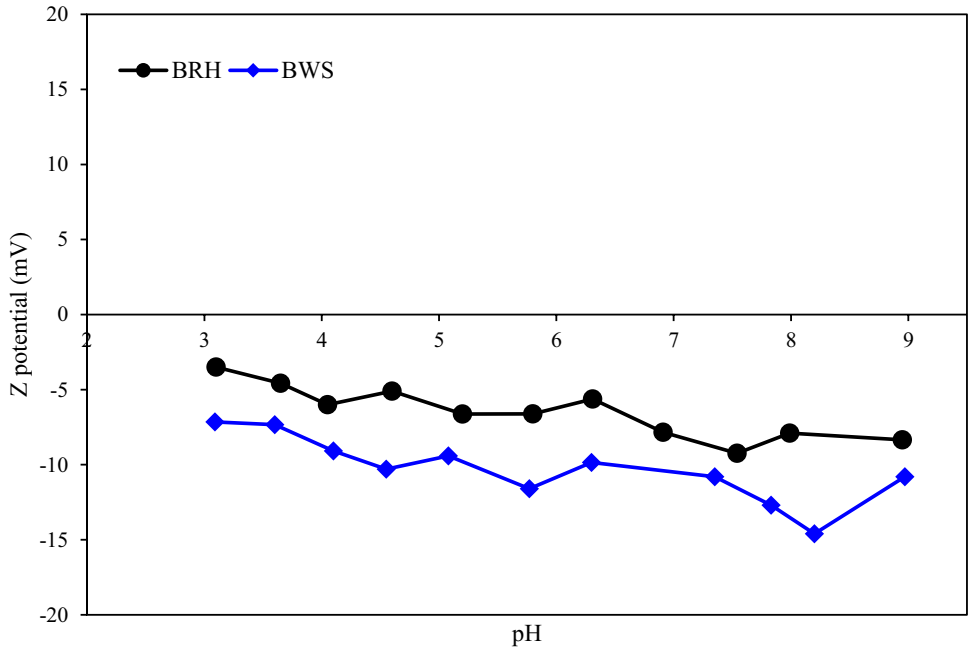

Fig. 4 Zeta potentials of biochars BRH and BWS under different pH values

zeta potential, and high porous size (instead of lower total porosity). Similar to the results obtained, Rubio-Clemente et al. [40] obtained MG removal capacity of 84.60% at the equilibrium point (30 min) when using palletized pine wood biochar. Pathy et al. [22] obtained a removal efficiency of 80% MG in the first 60 min of the sorption process when using algae biochar. However, the equilibrium point was reached at 180 min with a removal efficiency of 80 to 85%. In contrast, Tsai et al. [45] reported a maximum removal capacity of MG dye of 22.86% after 120 min of reaction when using rice husk biochar. On the other hand, 82.79% and 82.36% removal of As (III) was observed using BRH and BWS, respectively. Previous studies reported similar results for arsenic removal efficiency, specifically arsenite. Sattar et al. [46] reported that sorption was achieved at 120 min (equilibrium point) with 90% removal when using peanut shell biochar. Also, Ali et al. [47] reported removing up to 84% of As (III) when using almond shell biochar.

Table 3 shows the relevant kinetic parameters and correlation coefficients for MG and As (III) sorption on each

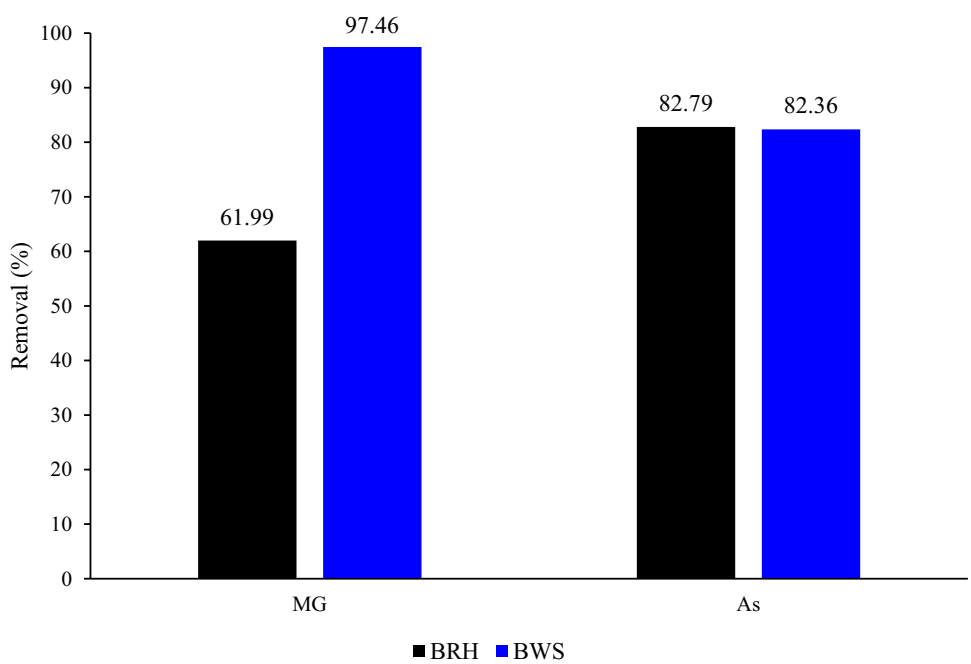

Fig. 5 Comparison of the removal efficiency of MG dye and As (III) by BRH and BWS at 120 min

Content courtesy of Springer Nature, terms of use apply. Rights reserved.

Table 3 Kinetic parameters for MG dye and As (III) sorption on each biochars (BRH/BWS)

Sample	$q_{e,\,exp}$ (mg g^{-1})	Pseudo-first-order			Pseudo-second-order		
		$q_{e,\,cal}$ (mg g^{-1})	k_1 (min^{-1})	R^2	$q_{e,\,cal}$ (mg g^{-1})	k_2 (g/mg·min)	R^2
MG/BRH	18.57	15.14	0.0141	0.828	18.64	0.00046	0.922
MG/BWS	29.19	28.00	0.0267	0.784	29.18	0.148	1
As/BRH	24.84	23.73	0.0259	0.39	24.85	0.336	1
As/BWS	24.80	24.71	0.0464	0.99	24.69	5.467	1

biochar sample employing the pseudo-first-order (PFO) and pseudo-second-order (PSO) kinetic models. The linearization indicates the correlation coefficient (R^2) values for the sorption kinetics fitted better to PSO ($R^2{}_{@BRH} = 0.922$ and $R^2{}_{@BWS} = 1$) than to PFO ($R^2{}_{@BRH} = 0.828$ and $R^2{}_{@BWS} = 0.784$) suggesting that the sorption of MG on both biochars occurred by the chemisorption mechanism. In the case of arsenite, the correlation coefficient (R^2) values were best fitted to PSO, suggesting that arsenic sorption on both biochars also occurs by the chemisorption mechanism. Therefore, chemisorption was found to be the rate-determining step, which controls the sorption of MG, and as for As (III), possibly both mechanisms (chemisorption and physisorption) were exhibited on biochars.

The sorption process involves a combination of diverse types of interactions between biochar and sorbate.

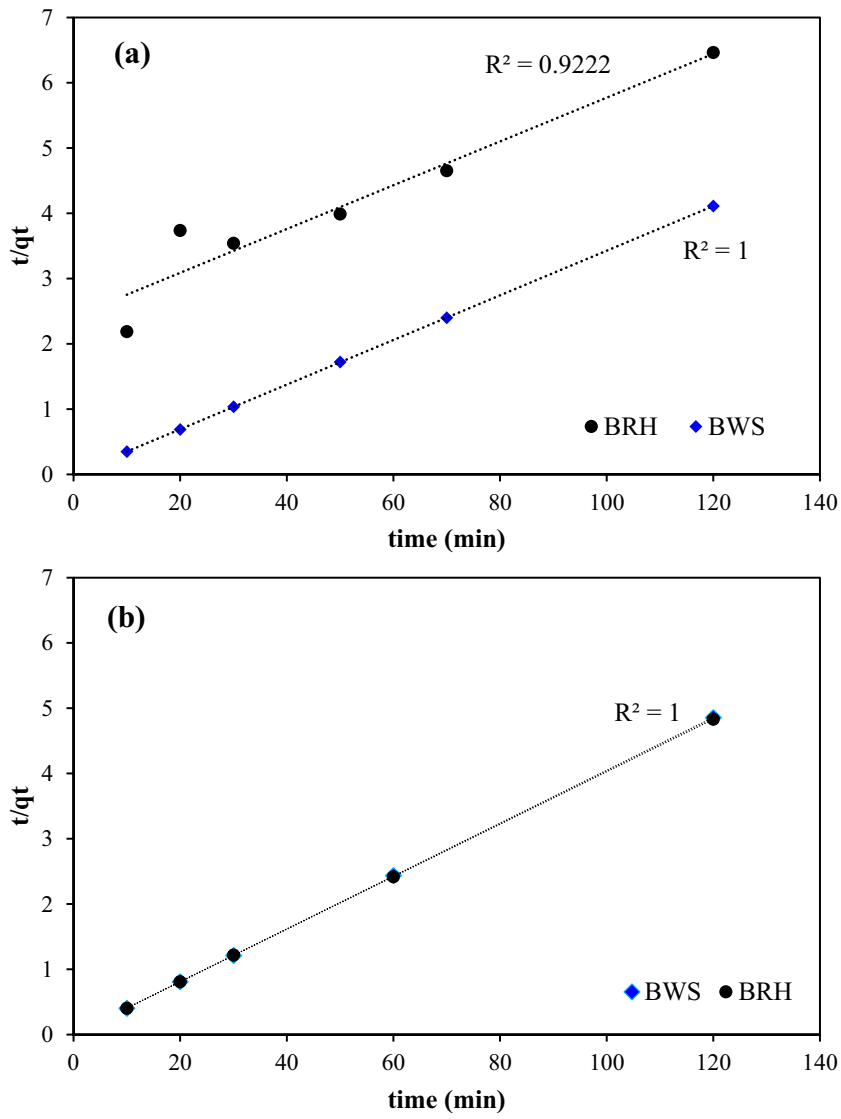

Fig. 6 (t/q_t) versus t. For **a** MG and **b** As (III), linearization of PSO

Content courtesy of Springer Nature, terms of use apply. Rights reserved.

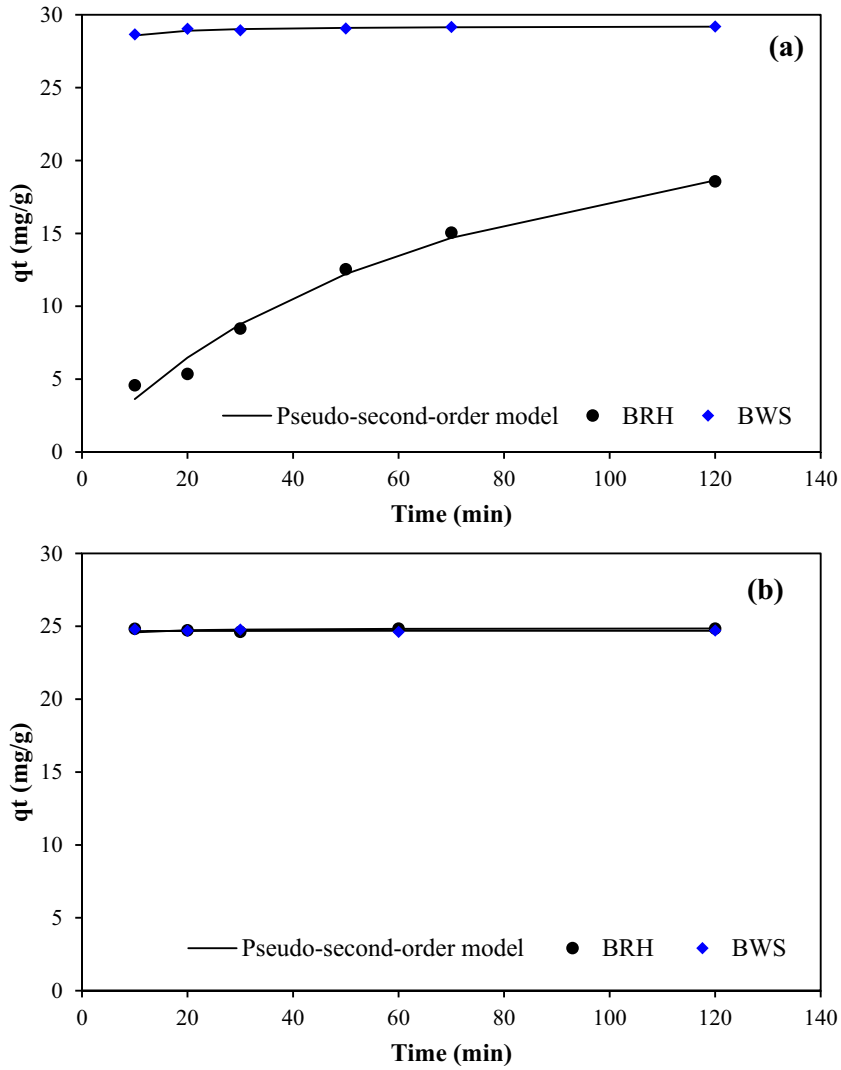

Fig. 7 Pseudo-second-order kinetic model. **a** MG. **b** As (III). Initial concentrations = 30 mg/L, 250 mg of biochars (BRH and BWS), 250 mL of volume, and room temperature

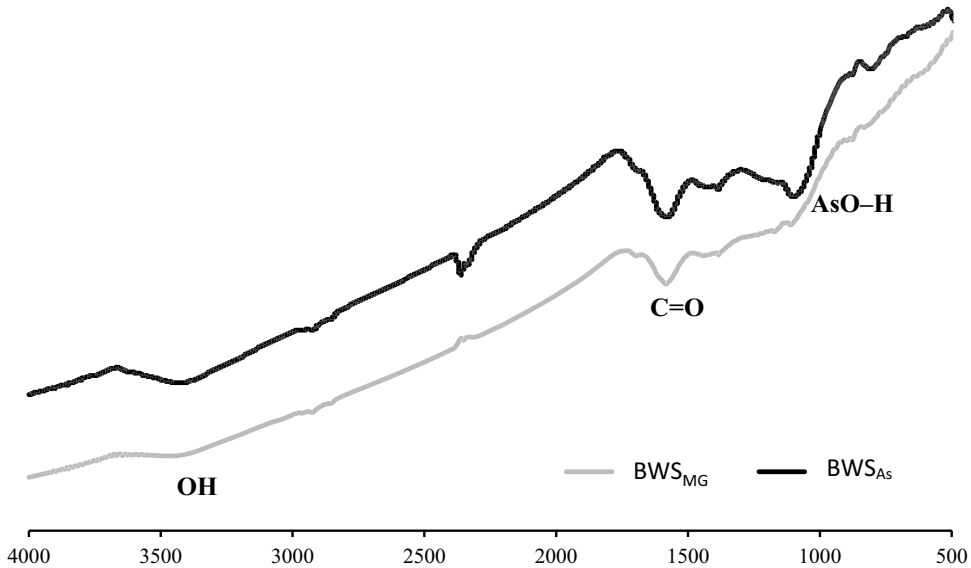

Fig. 8 FTIR analysis post-sorption of BWS_{MG} and BWS_{As}

Content courtesy of Springer Nature, terms of use apply. Rights reserved.

Table 4 Z potential and hydrodynamic diameter analysis post-sorption of BWS_{MG} and BWS_{As}

Sample	pH	Z potential (mV)	Hydrodynamic diameter (nm)	PDI
BWS	7.83	−12.7	1254	1
BWS_{MG}	7.54	−7.67	1751	1
BWS_{As}	7.55	−8.42	1563	1

Electrostatic interaction, ion exchange, complexation, and precipitation are the main mechanisms involved in the sorption of inorganic contaminants such as arsenic [48]. For organic contaminants such as MG, different mechanisms involved in sorption are observed, such as hydrogen bonding interaction, pore filling, electrostatic interaction, and π-π interactions [48, 49]. In addition, the sorption mechanism depends mainly on factors such as porosity, specific surface area, pH value, and functional groups on the surface of biochar [50]. Different studies attributed that the functional groups on the surface of biochar (-OH, -COOH, thiol (-SH), phenolic) strongly attract As [51] and MG [24, 52] through the sorption mechanism.

Figure 6 represents the plot of t/qt versus t showing a linear relationship. Values of equilibrium sorption capacity q_e and k_2 were calculated from the intercept and slope of the plot. Figure 7 shows that the experimental sorption capacity for both samples fits better than theoretical sorption capacity for the case of PSO, indicating that the sorption process follows the pseudo-second-order kinetic model.

3.7 FTIR and Z potential analysis of BWS samples after sorption of MG and arsenite

To verify the sorption mechanisms, FTIR analysis of BWS sample after sorption of MG and As (III) was performed (Fig. 8). BWS biochar showed an evident weakening in the band related to O–H bonds in As post-sorption material (BWS_{As}), related to carboxylic and hydroxylic groups (3000–3500 cm^{-1}) that indicate the contribution of OH groups in the uptake of As (III). Additionally, the C = O stretching bands were shifted to higher wavelengths suggesting chemical interactions between the As (III) and the surface functional groups, such as surface complexation, precipitation, and electrostatic interactions [46, 53, 54]. Finally, the new bands at peaks at 1380 and 1070–1100 cm^{-1} were related to the adsorbed arsenite (AsO–H) [55]. Furthermore, as can be observed in Fig. 8, similarly, there is an evident weakening of the O–H band found between 3000 and 3500 cm^{-1} in the MG post-sorption biochar spectra (BWS_{MG}). This fact indicates that there might be a strong sorption mechanism, such as a chemical bond through electron sharing between the nitrogen part of the amine functional group in the MG structure and the O–H functional group in the biochar [53, 56].

Table 4 shows the zeta potential and hydrodynamic diameter of BWS post-sorption of As (III) and MG. As observed, the Z potential of BWS biochar increases to less negative zeta potential values with the sorption of MG and As (III). This difference between the zeta potential of BWS and the post-sorption material suggests that MG and As (III) molecules had been attached to the BWS sorbent. It is noticed that hydrodynamic diameter increases; nevertheless, the polydispersity index is 1, which indicates that the samples are heterogeneous in size, which can be due to their agglomeration or aggregation.

4 Conclusions

Biochars obtained as by-products of rice husks and wild sugarcane gasification showed adequate characteristics to be used as sorbent of malachite green and arsenic from water solutions. The main conclusions are summarized as follows:

Sorption capacity values of biochars were 18.57 and 29.19 $mg \cdot g^{-1}$ for MG dye and 24.84 and 24.71 $mg \cdot g^{-1}$ for arsenite.

Both biochars showed fast sorption kinetics reaching equilibrium at 120 min and, in turn, resulted in a high sorption capacity, with an initial concentration of 30 $mg \cdot L^{-1}$ of both sorbates. The fits of the kinetic results indicated more accurately that the pseudo-second-order model best describes the sorption of two biochars, suggesting that the removal of MG dye and arsenite mainly supported the chemisorption. Moreover, according to post-sorption analysis, the functional groups -OH, C = O, and C = C were involved in the sorption of MG dye and arsenite on biochar. From the characterization data, it was observed that biochar obtained as by-product of wild sugarcane gasification is the biochar with the highest sorption capacity. This can be attributed to the combination of properties: functional groups, elemental composition, zeta potential, and cation exchange capacity.

Acknowledgements This research has been funded by Ministerio de Ciencia, Innovación y Universidades (MCIU), Agencia Estatal de Investigación (AEI), and Fondo Europeo de Desarrollo Regional (FEDER) with grant number RTI2018-096695-B-C31 and by Secretaría Nacional de Ciencias, Tecnología e Innovación (SENACYT), grant number 66-2019-ITE18-R2-016, project title: Carbonización de Biomasa: Aprovechamiento de Residuos Agrícolas para el Mejoramiento de las Propiedades Físico-químicas del Suelo en Áreas de Cultivo, and Sistema Nacional de Investigación (SNI) from the Republic of Panama. We thank the Ministerio de Ciencia, Innovación y Universidades (MCIU) and Agencia Estatal de Investigación (AEI) of Spain, the Fondo Europeo de Desarrollo Regional (FEDER), and the Secretaría Nacional de Ciencia, Tecnología e Innovación (SENACYT) of the Republic of Panama for its commitment and financial support.

Author contribution Yorgelis Barria: conceptualization; data curation; formal analysis; visualization; validation methodology; investigation; writing original draft; writing-review and editing.

Content courtesy of Springer Nature, terms of use apply. Rights reserved.

Aura Burbano: conceptualization; data curation; formal analysis; visualization; validation methodology; investigation; writing original draft; writing-review and editing.

Arthur James: investigation; funding acquisition; supervision; writing original draft.

Gabriel Gascó: conceptualization; funding acquisition; investigation; methodology; project administration; resources; supervision; writing-review and editing.

Ana Méndez: conceptualization; funding acquisition; investigation; methodology; project administration; resources; supervision; writing-review and editing.

Funding Open Access funding provided thanks to the CRUE-CSIC agreement with Springer Nature. This research was funded by Ministerio de Ciencia, Innovación y Universidades (MCIU), Agencia Estatal de Investigación (AEI), and Fondo Europeo de Desarrollo Regional (FEDER) with grant number RTI2018-096695-B-C31 and by the Secretaría Nacional de Ciencia, Tecnología e Innovación (SENACYT) within the project code 66–2019-ITE18-R2-016, together with the Sistema Nacional de Investigación (SNI).

Data availability The authors confirm that the data supporting this study are available within the article. Additional or related information will be supplied by the corresponding author (email: anamaria.mendez@upm.es).

Declarations

Ethics approval All authors complied according with the ethical principles of the *Biomass Conversion and Biorefinery* journal.

Conflict of interest The authors declare no competing interests.

Open Access This article is licensed under a Creative Commons Attribution 4.0 International License, which permits use, sharing, adaptation, distribution and reproduction in any medium or format, as long as you give appropriate credit to the original author(s) and the source, provide a link to the Creative Commons licence, and indicate if changes were made. The images or other third party material in this article are included in the article's Creative Commons licence, unless indicated otherwise in a credit line to the material. If material is not included in the article's Creative Commons licence and your intended use is not permitted by statutory regulation or exceeds the permitted use, you will need to obtain permission directly from the copyright holder. To view a copy of this licence, visit http://creativecommons.org/licenses/by/4.0/.

References

1. Hasan MdK, Shahriar A, Jim KU (2019) Water pollution in Bangladesh and its impact on public health. Heliyon 5:e02145. https://doi.org/10.1016/j.heliyon.2019.e02145
2. Berberich J, Li T, Sahle-Demessie E (2019) Chapter 11 Biosensors for monitoring water pollutants: a case study with arsenic in groundwater. Sep Sci Technol 11:285–328. https://doi.org/10.1016/B978-0-12-815730-5.00011-9
3. Mahadevan H, Nimina PVM, Krishnan KA (2022) An environmental green approach for the effective removal of malachite green from estuarine waters using Pistacia vera L. shell-based active carbon. Sustain Water Resour Manag 8:38. https://doi.org/10.1007/s40899-022-00612-5
4. Dai Y, Zhang N, Xing C et al (2019) The adsorption, regeneration and engineering applications of biochar for removal organic pollutants: a review. Chemosphere 223:12–27. https://doi.org/10.1016/j.chemosphere.2019.01.161
5. Berradi M, Hsissou R, Khudhair M et al (2019) Textile finishing dyes and their impact on aquatic environs. Heliyon 5:e02711. https://doi.org/10.1016/j.heliyon.2019.e02711
6. EFSA Contam Panel (EFSA Panel on Contaminants in the Food Chain) (2016) Malachite green in food. EFSA J 14:4530. https://doi.org/10.2903/j.efsa.2016.4530
7. Ahmad AA, Ahmad MA, Yahaya NKEM, Karim J (2021) Adsorption of malachite green by activated carbon derived from gasified Hevea brasiliensis root. Arab J Chem 14:103104. https://doi.org/10.1016/j.arabjc.2021.103104
8. Liu X, Gao M, Qiu W et al (2019) Fe–Mn–Ce oxide-modified biochar composites as efficient adsorbents for removing As (III) from water: adsorption performance and mechanisms. Environ Sci Pollut Res 26:17373–17382. https://doi.org/10.1007/s11356-019-04914-8
9. Ruíz-Huerta EA, de la Garza VA, Gómez-Bernal JM et al (2017) Arsenic contamination in irrigation water, agricultural soil and maize crop from an abandoned smelter site in Matehuala, Mexico. J Hazard Mater 339:330–339. https://doi.org/10.1016/j.jhazmat.2017.06.041
10. Sandil S, Óvári M, Dobosy P et al (2021) Effect of arsenic-contaminated irrigation water on growth and elemental composition of tomato and cabbage cultivated in three different soils, and related health risk assessment. Environ Res 197:111098. https://doi.org/10.1016/j.envres.2021.111098
11. World Health Organization (2017) Guidelines for drinking-water quality: fourth edition incorporating the first addendum. World Health Organization, Geneva
12. Alkurdi SSA, Al-Juboori RA, Bundschuh J et al (2021) Inorganic arsenic species removal from water using bone char: a detailed study on adsorption kinetic and isotherm models using error functions analysis. J Hazard Mater 405:124112. https://doi.org/10.1016/j.jhazmat.2020.124112
13. Guisela BZ, DA Ohana N, Dalvani SD et al (2022) Adsorption of arsenic anions in water using modified lignocellulosic adsorbents. Results Eng 13:100340. https://doi.org/10.1016/j.rineng.2022.100340
14. Yee JJ, Arida CVJ, Futalan CM et al (2019) Treatment of contaminated groundwater via arsenate removal using chitosan-coated bentonite. Molecules 24:1–16. https://doi.org/10.3390/molecules24132464
15. Nguyen KT, Navidpour AH, Ahmed MB et al (2022) Adsorption and desorption behavior of arsenite and arsenate at river sediment-water interface. J Environ Manage 317:115497. https://doi.org/10.1016/j.jenvman.2022.115497
16. Nnaji PC, Anadebe VC, Ezemagu IG, Onukwuli OD (2022) Potential of Luffa cylindrica seed as coagulation-flocculation (CF) agent for the treatment of dye wastewater: kinetic, mass transfer, optimization and CF adsorption studies. Arab J Chem 15:103629. https://doi.org/10.1016/j.arabjc.2021.103629
17. Kumar SA, Jarvin M, Inbanathan SSR et al (2022) Facile green synthesis of magnesium oxide nanoparticles using tea (Camellia sinensis) extract for efficient photocatalytic degradation of methylene blue dye. Environ Technol Innov 28:102746. https://doi.org/10.1016/j.eti.2022.102746
18. Moreira VR, Lebron YAR, Santos LVS et al (2021) Arsenic contamination, effects and remediation techniques: a special look onto membrane separation processes. Process Saf Environ Prot 148:604–623. https://doi.org/10.1016/j.psep.2020.11.033
19. Bhat SA, Bashir O, UlHaq SA et al (2022) Phytoremediation of heavy metals in soil and water: an eco-friendly, sustainable and multidisciplinary approach. Chemosphere 303:134788. https://doi.org/10.1016/j.chemosphere.2022.134788
20. Roy DC, Biswas SK, Sheam MdM et al (2020) Bioremediation of malachite green dye by two bacterial strains isolated from textile

Content courtesy of Springer Nature, terms of use apply. Rights reserved.

effluents. Curr Res Microb Sci 1:37–43. https://doi.org/10.1016/j.crmicr.2020.06.001
21. Wang H, Yuan X, Zeng G et al (2014) Removal of malachite green dye from wastewater by different organic acid-modified natural adsorbent: kinetics, equilibriums, mechanisms, practical application, and disposal of dye-loaded adsorbent. Environ Sci Pollut Res 21:11552–11564. https://doi.org/10.1007/s11356-014-3025-2
22. Pathy A, Krishnamoorthy N, Chang SX, Paramasivan B (2022) Malachite green removal using algal biochar and its composites with kombucha SCOBY: an integrated biosorption and phycoremediation approach. Surf Interfaces 30:101880. https://doi.org/10.1016/j.surfin.2022.101880
23. Sackey EA, Song Y, Yu Y, Zhuang H (2021) Biochars derived from bamboo and rice straw for sorption of basic red dyes. PLOS ONE 16:e0254637. https://doi.org/10.1371/journal.pone.0254637
24. El Hadj A, Ali Y, Ahrouch M, Ait Lahcen A et al (2022) Recent advances and prospects of biochar-based adsorbents for malachite green removal: a comprehensive review. Chem Afr. https://doi.org/10.1007/s42250-022-00391-8
25. Bethancourt G, James A, Villarreal JE, Marin-Calvo N (2019) Biomass carbonization - production and characterization of biochar from rice husks. 2019 7th International Engineering, Sciences and Technology Conference (IESTEC). IEEE, Panama, pp 40–45
26. Gascó G, Álvarez ML, Paz-Ferreiro J et al (2018) Valorization of biochars from pinewood gasification and municipal solid waste torrefaction as peat substitutes. Environ Sci Pollut Res 25:26461–26469. https://doi.org/10.1007/s11356-018-2703-x
27. James RAM, Yuan W, Boyette MD, Wang D (2018) Airflow and insulation effects on simultaneous syngas and biochar production in a top-lit updraft biomass gasifier. Renew Energy 117:116–124. https://doi.org/10.1016/j.renene.2017.10.034
28. Chen Y, Zhu Y, Wang Z et al (2011) Application studies of activated carbon derived from rice husks produced by chemical-thermal process—a review. Adv Colloid Interface Sci 163:39–52. https://doi.org/10.1016/j.cis.2011.01.006
29. Saltonstall K, Bonnett GD, Aitken KS (2021) A perfect storm: ploidy and preadaptation facilitate Saccharum spontaneum escape and invasion in the Republic of Panama. Biol Invasions 23:1101–1115. https://doi.org/10.1007/s10530-020-02421-3
30. Alaín DN, Pérez JJL, Aguilar G. OA (2019) Wild sugarcane (Saccharum spontaneum) invasive herbaceous species as a potential energy resource in Panama. 2019 7th Int Eng Sci Technol Conf IESTEC 203–208. https://doi.org/10.1109/IESTEC46403.2019.00-75
31. Chen J, James Rivas A, Deago E, et al. (2021) CASO VIII. Implementación de Saccharum spontaneum L. como materia prima en el tratamiento de aguas contaminadas. 169
32. Rodríguez L, Deago E, Cueto G, Jaramillo A (2021) Saccharum spontaneum L. Evaluada como Sustrato sólido orgánico natural en Desnitrificación biológica. Congr Nac Cienc Tecnol – APANAC 197–204. https://doi.org/10.33412/apanac.2021.3184
33 Prens J, Kurt Z, James Rivas AM, Chen J (2022) Production and characterization of wild sugarcane (Saccharum spontaneum L.) biochar for atrazine adsorption in aqueous media. Agronomy 13:27. https://doi.org/10.3390/agronomy13010027
34. James RAM, Yuan W, Boyette DM et al (2016) Characterization of biochar from rice hulls and wood chips produced in a top-lit updraft biomass gasifier. Trans ASABE 59:749–756. https://doi.org/10.13031/trans.59.11631
35. Thomas GW (1996) Soil pH and soil acidity. Methods Soil Anal 475–490. https://doi.org/10.2136/sssabookser5.3.c16
36. Rhoades JD (1996) Salinity: electrical conductivity and total dissolved solids. Methods Soil Anal 19. https://doi.org/10.2136/sssabookser5.3.c14
37. Navarro AF, Cegarra J, Roig A, Garcia D (1993) Relationships between organic matter and carbon contents of organic wastes. Bioresour Technol 44:203–207. https://doi.org/10.1016/0960-8524(93)90153-3
38. ISO 23470 (2007) Soil quality - determination of effective cation exchange capacity (CEC) and exchangeable cations using a hexamminecobalt trichloride solution
39. Kajjumba GW, Emik S, Öngen A et al (2018) Modelling of adsorption kinetic processes—errors, theory and application. Adv Sorpt Process Appl. https://doi.org/10.5772/intechopen.80495
40. Rubio-Clemente A, Gutiérrez J, Henao H, et al. (2021) Adsorption capacity of the biochar obtained from Pinus patula wood microgasification for the treatment of polluted water containing malachite green dye. J King Saud Univ - Eng Sci S1018363921000982. https://doi.org/10.1016/j.jksues.2021.07.006
41. Cha JS, Park SH, Jung S-C et al (2016) Production and utilization of biochar: a review. J Ind Eng Chem 40:1–15. https://doi.org/10.1016/j.jiec.2016.06.002
42. Xiang W, Zhang X, Chen J et al (2020) Biochar technology in wastewater treatment: a critical review. Chemosphere 252:126539. https://doi.org/10.1016/j.chemosphere.2020.126539
43. Peterson SC, Jackson MA (2014) Simplifying pyrolysis: using gasification to produce corn stover and wheat straw biochar for sorptive and horticultural media. Ind Crops Prod 53:228–235. https://doi.org/10.1016/j.indcrop.2013.12.028
44. Hansen V, Müller-Stöver D, Ahrenfeldt J et al (2015) Gasification biochar as a valuable by-product for carbon sequestration and soil amendment. Biomass Bioenergy 72:300–308. https://doi.org/10.1016/j.biombioe.2014.10.013
45. Tsai C-Y, Lin P-Y, Hsieh S-L et al (2022) Engineered mesoporous biochar derived from rice husk for efficient removal of malachite green from wastewaters. Bioresour Technol 347:126749. https://doi.org/10.1016/j.biortech.2022.126749
46. Sattar MS, Shakoor MB, Ali S et al (2019) Comparative efficiency of peanut shell and peanut shell biochar for removal of arsenic from water. Environ Sci Pollut Res 26:18624–18635. https://doi.org/10.1007/s11356-019-05185-z
47. Ali S, Rizwan M, Shakoor MB et al (2019) High sorption efficiency for As(III) and As(V) from aqueous solutions using novel almond shell biochar. Chemosphere 243:125330. https://doi.org/10.1016/j.chemosphere.2019.125330
48. Abbas Z, Ali S, Rizwan M et al (2018) A critical review of mechanisms involved in the adsorption of organic and inorganic contaminants through biochar. Arab J Geosci 11:448. https://doi.org/10.1007/s12517-018-3790-1
49. Ambaye TG, Vaccari M, van Hullebusch ED et al (2021) Mechanisms and adsorption capacities of biochar for the removal of organic and inorganic pollutants from industrial wastewater. Int J Environ Sci Technol 18:3273–3294. https://doi.org/10.1007/s13762-020-03060-w
50. Jha S, Gaur R, Shahabuddin S, Tyagi I (2023) Biochar as sustainable alternative and green adsorbent for the remediation of noxious pollutants: a comprehensive review. Toxics 11:117. https://doi.org/10.3390/toxics11020117
51. Srivastav AL, Pham TD, Izah SC et al (2022) Biochar adsorbents for arsenic removal from water environment: a review. Bull Environ Contam Toxicol 108:616–628. https://doi.org/10.1007/s00128-021-03374-6
52. Abate GY, Alene AN, Habte AT, Getahun DM (2020) Adsorptive removal of malachite green dye from aqueous solution onto activated carbon of Catha edulis stem as a low cost bioadsorbent. Environ Syst Res 9:29. https://doi.org/10.1186/s40068-020-00191-4
53. Park J-H, Lee J-H, Lee S-L et al (2021) Adsorption behavior of arsenic onto lignin-based biochar decorated with zinc. Colloids Surf Physicochem Eng Asp 626:127095. https://doi.org/10.1016/j.colsurfa.2021.127095
54. Li H, Dong X, da Silva EB et al (2017) Mechanisms of metal sorption by biochars: biochar characteristics and modifications.

Content courtesy of Springer Nature, terms of use apply. Rights reserved.

Chemosphere 178:466–478. https://doi.org/10.1016/j.chemosphere.2017.03.072
55. Bahfenne S, Frost RL (2010) A review of the vibrational spectroscopic studies of arsenite, antimonite, and antimonate minerals. Appl Spectrosc Rev 45:101–129. https://doi.org/10.1080/05704920903435839
56 Omar H, EL-Gendy A, AL-Ahmary K (2018) Bioremoval of toxic dye by using different marine macroalgae. Turk J Bot 42:15–27. https://doi.org/10.3906/bot-1703-4

Publisher's note Springer Nature remains neutral with regard to jurisdictional claims in published maps and institutional affiliations.

Content courtesy of Springer Nature, terms of use apply. Rights reserved.

Terms and Conditions

Springer Nature journal content, brought to you courtesy of Springer Nature Customer Service Center GmbH ("Springer Nature").

Springer Nature supports a reasonable amount of sharing of research papers by authors, subscribers and authorised users ("Users"), for small-scale personal, non-commercial use provided that all copyright, trade and service marks and other proprietary notices are maintained. By accessing, sharing, receiving or otherwise using the Springer Nature journal content you agree to these terms of use ("Terms"). For these purposes, Springer Nature considers academic use (by researchers and students) to be non-commercial.

These Terms are supplementary and will apply in addition to any applicable website terms and conditions, a relevant site licence or a personal subscription. These Terms will prevail over any conflict or ambiguity with regards to the relevant terms, a site licence or a personal subscription (to the extent of the conflict or ambiguity only). For Creative Commons-licensed articles, the terms of the Creative Commons license used will apply.

We collect and use personal data to provide access to the Springer Nature journal content. We may also use these personal data internally within ResearchGate and Springer Nature and as agreed share it, in an anonymised way, for purposes of tracking, analysis and reporting. We will not otherwise disclose your personal data outside the ResearchGate or the Springer Nature group of companies unless we have your permission as detailed in the Privacy Policy.

While Users may use the Springer Nature journal content for small scale, personal non-commercial use, it is important to note that Users may not:

1. use such content for the purpose of providing other users with access on a regular or large scale basis or as a means to circumvent access control;
2. use such content where to do so would be considered a criminal or statutory offence in any jurisdiction, or gives rise to civil liability, or is otherwise unlawful;
3. falsely or misleadingly imply or suggest endorsement, approval , sponsorship, or association unless explicitly agreed to by Springer Nature in writing;
4. use bots or other automated methods to access the content or redirect messages
5. override any security feature or exclusionary protocol; or
6. share the content in order to create substitute for Springer Nature products or services or a systematic database of Springer Nature journal content.

In line with the restriction against commercial use, Springer Nature does not permit the creation of a product or service that creates revenue, royalties, rent or income from our content or its inclusion as part of a paid for service or for other commercial gain. Springer Nature journal content cannot be used for inter-library loans and librarians may not upload Springer Nature journal content on a large scale into their, or any other, institutional repository.

These terms of use are reviewed regularly and may be amended at any time. Springer Nature is not obligated to publish any information or content on this website and may remove it or features or functionality at our sole discretion, at any time with or without notice. Springer Nature may revoke this licence to you at any time and remove access to any copies of the Springer Nature journal content which have been saved.

To the fullest extent permitted by law, Springer Nature makes no warranties, representations or guarantees to Users, either express or implied with respect to the Springer nature journal content and all parties disclaim and waive any implied warranties or warranties imposed by law, including merchantability or fitness for any particular purpose.

Please note that these rights do not automatically extend to content, data or other material published by Springer Nature that may be licensed from third parties.

If you would like to use or distribute our Springer Nature journal content to a wider audience or on a regular basis or in any other manner not expressly permitted by these Terms, please contact Springer Nature at

onlineservice@springernature.com